NeuroScanAI: Segmentation and classification of tumors in MRI Brain Images

Hasaan Maqsood [1] **Inna Larina** [1] **Iana Kulichenko** [1]

Abstract

Brain tumors are a critical health issue that significantly affects patients' quality of life and survival rates. Precise segmentation and classification of brain tumors from MRI images are essential for effective treatment planning, yet the current reliance on manual analysis by specialists is both time-consuming and subject to human error. This research proposes the development and evaluation of automated computer-based algorithms, leveraging advanced deep learning techniques, to address these challenges. Our aim is to bridge the gap in diagnostic accuracy and efficiency caused by the heterogeneity of tumor appearances and the complexities inherent in MRI data.

This study will investigate a range of deep learning models, adopting an exploratory approach to identify the most efficacious methods for accurate tumor segmentation and classification. The goal is to significantly enhance diagnostic speed and reliability, thereby supporting more informed clinical decision-making and optimizing both treatment planning and efficacy monitoring.

By applying cutting-edge computational techniques to a pressing healthcare problem, this project seeks to contribute substantially to the fight against brain tumors. Expected outcomes include the development of a scalable and efficient tool for the medical community, potentially improving patient management and prognoses by offering a pathway to more personalized and timely treatment options.

Github repo: Please click here to see our project repo.
Presentation: Our Presentation.

[1]Skolkovo Institute of Science and Technology, Moscow, Russia. Correspondence to: Hasaan Maqsood <hasaan.maqsood@skoltech.ru>, Inna Larina <inna.larina@skoltech.ru>, Iana Kulichenko <Iana.Kulichenko@skoltech.ru>.

Final Projects of the Machine Learning 2020 Course, Skoltech, Moscow, Russian Federation, 2020.

1. Introducion

Tumors represent a significant health concern due to their varied impact on the human body, categorized broadly into benign (non-cancerous) and malignant (cancerous) types. Their nature and behavior differ vastly, with malignant tumors possessing the potential for aggressive growth and metastasis, thus necessitating precise diagnostic and treatment strategies.

Among the numerous methods available for tumor diagnosis, Magnetic Resonance Imaging (MRI) stands out for its ability to provide high-resolution images of soft tissues, including brain tumors, without invasive intervention. This capability is crucial for identifying the diverse types of tumors, such as gliomas and meningioma's, and for determining the appropriate course of treatment.

We focus on gliomas, meningiomas, and pituitary tumors, each distinct in origin and characteristics detectable through MRI imaging. Gliomas, arising from glial cells, exhibit varying signal intensities on MRI, with high-grade cases often showing ring-like enhancement and surrounding edema. Meningiomas, originating from the meninges, typically appear as well-defined, homogeneous masses on MRI scans, displacing rather than invading surrounding tissue. Pituitary tumors, located within the sella turcica, present as rounded masses near the optic chiasm with variable signal intensities and may exhibit features such as cystic changes or calcifications. While MRI aided by AI assists in detection and classification, the final diagnosis still relies on expert interpretation and histopathological examinations.

Traditionally, tumor diagnosis via MRI relies heavily on the expertise of radiologists, who manually interpret the imaging data to identify and classify tumors. This manual analysis, while invaluable, is marred by several limitations. Primarily, it is time-intensive and susceptible to inter-observer variability, leading to potential inconsistencies in diagnosis. Furthermore, the subtleties of tumor appearance in MRI scans can sometimes be overlooked, compromising diagnostic accuracy.

Deep learning, a subset of artificial intelligence, has recently been heralded as a transformative solution to the challenges of traditional diagnostic methods. By utilizing algorithms that can learn from data, deep learning models, particularly

Convolutional Neural Networks (CNNs), have been applied to MRI data for automated tumor segmentation and classification. These methods have shown promise in enhancing diagnostic precision, reducing time, and minimizing observer variability.

In response to the existing challenges and building on the successes of current research, our study proposes a novel deep learning framework tailored for MRI-based tumor diagnosis. Our method aims to leverage the strengths of deep learning to offer greater diagnostic accuracy, efficiency, and consistency. By incorporating cutting-edge model architectures and training methodologies, we intend to advance the state-of-the-art in tumor classification and segmentation, addressing the limitations of both manual analysis and existing automated approaches.

2. Literature Review

Existing studies in MRI brain image segmentation and tumor classification have demonstrated notable advancements. Ma et al. (1). introduced MedSAM, a model designed for universal medical image segmentation, showcasing superior accuracy across diverse imaging modalities. Xu et al.(2) presented an automatic glioma segmentation approach using the UNet++ model, enhancing diagnosis and treatment planning. Hafeez et al (3). proposed a lightweight CNN for glioma grading classification, achieving high accuracy on benchmarked datasets. Khan et al (4). developed ensemble frameworks for brain tumor prediction, showing promising results in early detection. Saeedi et al (5). explored deep learning and machine learning techniques for brain tumor detection using MRI images. Chatterjee et al.'s. (6). research demonstrated that spatiotemporal deep learning models, specifically Pre-trained ResNet Mixed Convolution, significantly outperform traditional 3D models in MRI-based brain tumour classification, achieving a macro F1-score of 0.9345 and a 96.98% accuracy with reduced computational costs. David N Louis et al.'s. (7). Provides an overview of the fifth edition of the WHO Classification of Tumors of the Central Nervous System (CNS), highlighting major changes and advancements in CNS tumor classification. Incorporates molecular biomarkers for more accurate classification, alongside histological and immunohistochemical approaches. Introduces new tumor types and subtypes, including those based on novel diagnostic technologies such as DNA methylome profiling. Aggarwal et al.'s (8) propose a method for early detection and segmentation of brain tumors using Deep Neural Networks (DNN). Utilizes an Improved Residual Network (ResNet) to overcome gradient diffusion issues in DNN training. Achieves competitive performance over traditional methods with more than 10% improved accuracy, recall, and f-measure. Chandan et al.'s (9). work on fully automated deep learning method for brain tumor segmentation, utilizing 285 cases from the BraTS2018 dataset and employing 3D-Dense-UNets for binary segmentation of tumor subcomponents. The method demonstrated high accuracy, with mean Dice-scores of 0.92 (WT), 0.84 (TC), and 0.80 (ET) across various validation sets, showing its potential for clinical workflow integration. This approach simplifies complex multiclass segmentation by effectively generalizing network performance through 3-fold cross-validation. Mina Ghaffari et at. 's (10). review the evolution of automated models for brain tumor segmentation using multimodal MR images. In order to be able to make a just comparison between different methods, the proposed models are studied for the most famous benchmark for brain tumor segmentation, namely the BraTS challenge.

While these studies have made significant contributions, there are still gaps in the literature. Some limitations include challenges in achieving high accuracy across different tumor types and imaging modalities, as well as the need for more comprehensive evaluation on diverse datasets. Additionally, there is a lack of studies focusing on the integration of multiple imaging modalities for improved tumor detection and classification.

The theoretical framework underlying our research involves machine learning algorithms, particularly convolutional neural networks (CNNs) and ensemble learning techniques. These models serve as the foundation for our approach to MRI brain image segmentation and tumor classification.

Our research addresses the identified gaps in the literature by proposing an integrated approach that combines CNN-based segmentation with ensemble learning for tumor classification. By leveraging state-of-the-art techniques and methodologies, we aim to improve the accuracy and efficiency of brain tumor detection and classification, ultimately contributing to more effective diagnosis and treatment planning.

3. Proposed Methodology

3.1. Proposed method

We introduce a comparative analysis of Segmentation and Classification approaches. Firstly, we train segmentation models on the LGG segmentation dataset and classifiers on the classification dataset consisting of MRI images. Secondly, we predict segmentation masks for the classification dataset using selected segmentation model and overlay them with original MRI scans. Thirdly, we train classifiers again on the masked classification dataset.
Our hypothesis states that by the segmentation supplement we enhance classifiers performance in terms of the following metrics: accuracy, precision, recall and f1 score.

3.2. Dataset

3.2.1. LGG Segmentation Dataset Description

The dataset consists of MRI brain images paired with FLAIR abnormality segmentation masks derived from The Cancer Imaging Archive (TCIA). This collection features 110 cases from The Cancer Genome Atlas (TCGA) that include lower-grade glioma patients, each with corresponding FLAIR sequence imaging and genomic data. Detailed patient information and genomic cluster classifications are cataloged within the data.csv file.
Imaging data is presented in .tif format, with each image containing three channels. A majority of the cases (101 out of 110) provide a complete set of sequences: pre-contrast, FLAIR, and post-contrast. For the remaining cases, where either post-contrast (9 cases) or pre-contrast (6 cases) sequences are absent, the FLAIR sequence is replicated to ensure uniformity across all images as three-channel inputs. Segmentation masks are provided as binary, single-channel images that delineate the FLAIR-detected abnormalities.
The dataset is meticulously organized into 110 distinct folders, each named using a unique case ID that reflects the originating institution. Within these folders, the MRI scans and their respective masks adhere to a consistent naming convention: TCGA institution-code patient-id slice-number .tif, with the associated masks identified by an appended mask suffix.

In the dataset comprising a total of 3929 samples, we partitioned it into training, testing, and validation sets with a distribution of 2828, 393, and 708 samples, respectively, ensuring a structured approach for model training and evaluation.

The Cancer Genome Atlas
Center of cancer genomics

3.2.2. Classification Dataset

For classifying tumors in MRI brain images, we chose dataset from Kaggle. The Classification Dataset (11) has a split into test/train sets with the following categories: “glioma-tumor”, “meningioma-tumor”, “pituitary-tumor”, “no-tumor”. Image sizes vary up to 512x512 pixels and have a distinct shape.

3.3. Segmentation

3.3.1. Preprocessing

Data Acquisition:
The project utilizes the publicly available LGG MRI segmentation dataset from Kaggle, which contains MRI scans with corresponding segmentation masks. The dataset is downloaded using Kaggle’s API.

One-hot Encoding and Reverse Encoding:
Segmentation labels are one-hot encoded to transform categorical labels into a binary matrix representation, which is compatible with the output format expected by neural network models. A reverse one-hot encoding function is also provided to convert predictions back to the original label format for performance evaluation.

Custom Dataset Class:
The LGGDataset class is designed to handle the loading of images and masks, apply one-hot encoding, and perform augmentations and preprocessing steps. This class ensures that the data is correctly formatted and augmented before being fed into the segmentation model

Image Size Divisibility by 32: Ensuring image dimensions (height and width) are divisible by 32 is crucial for segmentation tasks. This requirement stems from the architecture of most segmentation models, like those in the SMP library, which feature skip-connections between encoder and decoder stages. With 5 downsampling stages in the encoder, input dimensions must be divisible by $2^5 = 32$ to ensure proper alignment of encoder and decoder features. Non-compliant image sizes can result in alignment errors, affecting segmentation performance.

Data Augmentation:
To enhance model generalization, data augmentation introduces training data variability. Techniques include *RandomCrop* (crops random 256x256 sections, focusing on varying regions), *HorizontalFlip* and *VerticalFlip* (flips images horizontally or vertically with a 0.8 probability, introducing variance), *RandomRotate90* (rotates images 90 degrees randomly with 0.8 probability for rotational variance), *CLAHE* (enhances local contrast, crucial for medical imaging), *RandomBrightnessContrast* and *RandomGamma* (adjusts brightness, contrast, and gamma with 0.5 probability, simulating different conditions), and *Normalize* (scales pixel values using ImageNet statistics for standardized input). Applied sequentially via Albumentations’ Compose, these augmentations ensure diverse and challenging training data.

3.3.2. Models

In our study, we employed the EfficientNetB5 neural network as the encoder for segmenting brain scans into two categories: healthy tissue and tumor presence. The selection of EfficientNetB5 was based on its optimal balance of complexity and performance, with its 28 million parameters providing a more efficient and effective solution compared to other architectures like ResNet, which were less efficient in our initial evaluations. For the segmentation task, we utilized a suite of models, including U-Net, U-Net++, Pyramid Attention Network (PAN), and DeepLabV3+. These models were fine-tuned using a set of augmentations comprising average pooling, a dropout rate of 0.3, and sigmoid activa-

tion to produce a binary segmentation output. We measured the segmentation quality using the Intersection over Union (IoU) metric, setting a threshold of 0.55 to evaluate the model's performance. The training and validation processes were conducted over 7 epochs on a CUDA-enabled device, which provided the necessary computational efficiency and memory optimization. Our approach was carefully designed to maximize the accuracy of differentiating between healthy and tumorous brain tissues, capitalizing on the robust capabilities of the EfficientNetB5 architecture and the advanced segmentation techniques implemented in our models.

U-Net:
Nested Skip Pathways: U-Net++ improves upon the original U-Net by introducing nested, dense skip pathways, which enhance the flow of information. This allows for better gradient flow and feature propagation, leading to more detailed segmentation results and potentially better performance in identifying tumor boundaries. Multi-scale Feature Aggregation: The architecture is designed to aggregate features at multiple scales, which can be particularly beneficial for capturing the heterogeneity of brain tumors that may appear at various sizes and shapes within MRI scans

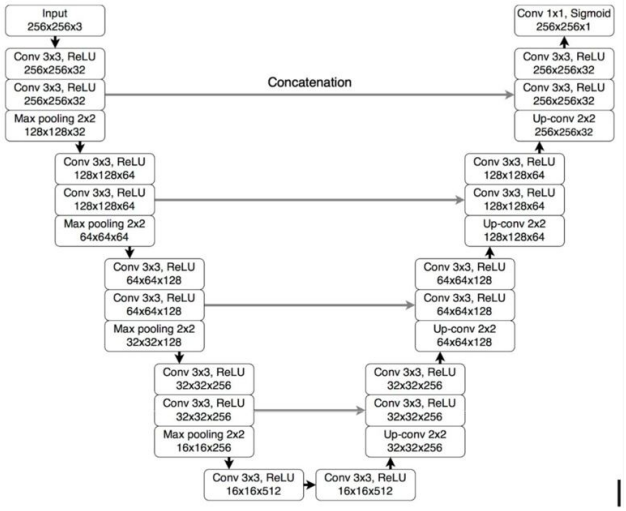

Figure 1. U-NET architecture

U-Net++:
Nested Skip Pathways: U-Net++ improves upon the original U-Net by introducing nested, dense skip pathways, which enhance the flow of information. This allows for better gradient flow and feature propagation, leading to more detailed segmentation results and potentially better performance in identifying tumor boundaries.
Multi-scale Feature Aggregation: The architecture is designed to aggregate features at multiple scales, which can be particularly beneficial for capturing the heterogeneity of brain tumors that may appear at various sizes and shapes within MRI scans.

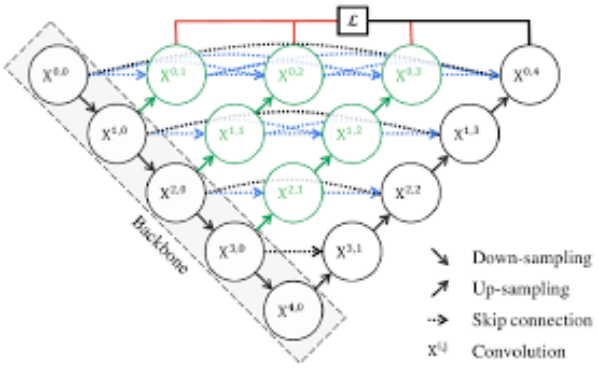

Figure 2. U-NET++ architecture

PAN (Pyramid Attention Network):
Attention Mechanisms: PAN uses attention mechanisms (Global Attention Upsample (GAU)) to focus on salient features that are relevant for the task at hand. In the case of brain tumor segmentation, the attention mechanism can help the model focus on the regions of interest, such as abnormal tissue, while suppressing less relevant background information.
Feature Pyramid Attention: This feature enables the model to capture contextual information at different scales, which is important for segmenting brain tumors that can vary greatly in size and appearance.

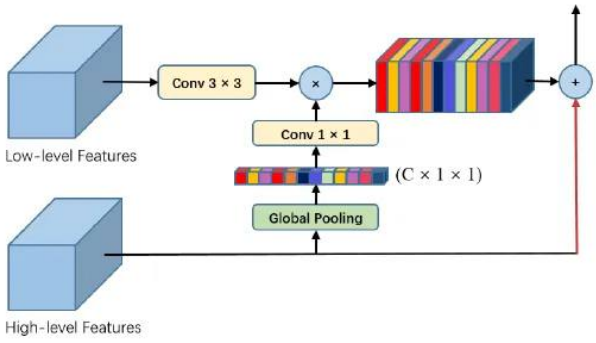

Figure 3. Global Attention Upsample architecture

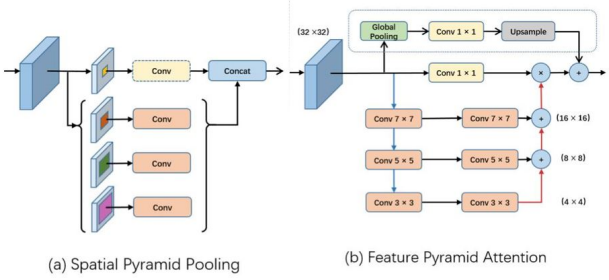

Figure 4. Feature Pyramid Attention module structure

DeepLabV3 and DeepLabV3+:
Atrous Convolutions: These models use atrous (dilated) convolutions to control the resolution at which feature responses are computed within CNNs. This allows the models to capture multi-scale information without increasing the number of parameters or the amount of computation.
ASPP (Atrous Spatial Pyramid Pooling): DeepLabV3 includes an ASPP module that probes an incoming convolutional feature layer with filters at multiple sampling rates and effective fields-of-view, capturing objects as well as image context at multiple scales.
Decoder Module: DeepLabV3+ adds a decoder module to refine the segmentation results, focusing on recovering the object boundaries. This is particularly useful for medical images where the distinction between healthy tissue and tumors may be subtle.

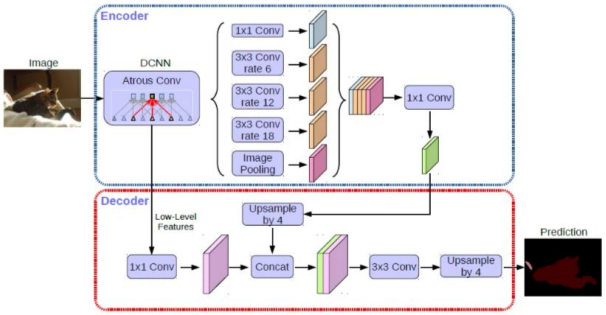

Figure 5. Encoder DeepLabv3, with decoder is DeepLabv3+ architecture

These models are particularly good for semantic segmentation tasks like brain tumor segmentation due to their ability to handle the variability in shape, size, and appearance of tumors within MRI images. They are capable of capturing both local and global contextual information, which is crucial for accurate segmentation. Moreover, their architectures are designed to preserve spatial information throughout the network, allowing for precise delineation of tumor boundaries, which is essential for subsequent analysis and treatment planning.

3.4. Classification

3.4.1. Preprocessing

Loading Dataset:
The Dataset is loaded from the folders with MRI images, which are downloaded from Kaggle.
Label Encoding:
Tumor categories “glioma-tumor”, “meningioma-tumor”, “pituitary-tumor”, “no-tumor” are encoded using simple Label Encoder from scikit-learn library.
Data Augmentation:
We applied data augmentation to increase the quality of MRI data. Random resized cropping, random rotation, random horizontal flipping, random affining, random perspective transformation, and normalization were applied to the train set, while center cropping, resizing, and normalization were applied to the test set within the classification task. It ensured better performance of the classifier. After the transformation step, the dataset was split into the train/test/validation set and sent to the dataloader.

3.4.2. Models

Selected classification models:
As a part of the classification task, we implement the following models: ResNet18, ResNet34, ResNet50, and EfficientNet. The training procedure is performed both using the original MRI images and the combination of MRI images with segmentation masks. To evaluate models’ performance we use the following metrics: accuracy, precision, recall, and f1 score.

Criterion and optimizer:
We use SGD optimizer and CrossEntropy loss-function, because for all models such configuration showed better performance. As a result of manual feature engineering the following hyperparameters for classification models were chosen:

Table 1. Classification Hyperparameters

Model	Lr rate	Momentum	Weig. decay
ResNet18	0.003	0.9	0.0001
ResNet34	0.008	0.7	0.001
ResNet50	0.008	0.7	0.0001
EfficientNet	0.005	0.7	0.001

4. Result Analysis

4.1. Segmentation results

The models’ performances are evaluated using the Intersection over Union (IoU) metric. The results are as follows:

Table 2. Segmentation Performance

Model	Train loss	Valid Loss	IOU
DeepLabV3+	1.6634	1.6662	0.8741
UNET	1.6691	1.6712	0.8517
UNET++	1.6730	1.6750	0.8268
DeepLabV3	1.6646	1.6700	0.7986
PAN	1.6656	1.6683	0.7970

DeepLabV3+ emerges as the top-performing model, indicating its superior capability in segmenting brain tumors from MRI images. The choice of models, loss functions, and evaluation metrics is driven by the objective to achieve high-precision segmentation, which is critical for the accurate diagnosis and treatment of brain tumors. The experimental

setup and results contribute valuable insights into the application of deep learning for medical image segmentation, with potential implications for enhancing clinical workflows and patient care.

Combined Loss Function:
The project employs a combined loss function that integrates Dice loss and Binary Cross-Entropy (BCE) loss. This hybrid approach is designed to leverage the strengths of both loss functions to address the challenges inherent in medical image segmentation. Dice Loss: For segmentation tasks, it measures the overlap between the predicted segmentation mask and the ground truth mask.Binary Cross-Entropy (BCE) Loss: BCE loss calculates the pixel-wise difference between the predicted probabilities and the actual binary labels in the ground truth.Combining Dice loss and BCE loss allows the model to simultaneously optimize for global structure similarity (via Dice loss) and local pixel accuracy (via BCE loss), leading to more precise and reliable segmentation results.

4.1.1. Performance Metrics

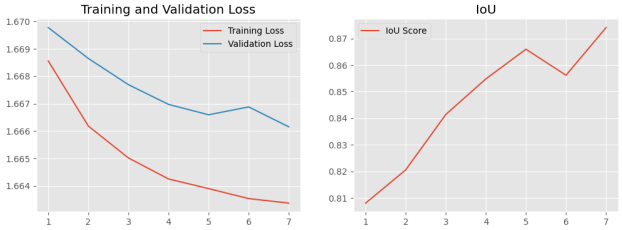

Figure 6. DeepLabV3+-Result

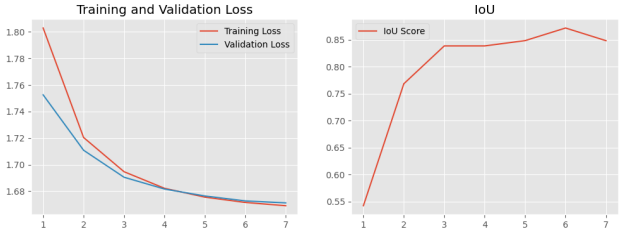

Figure 7. UNet-Results

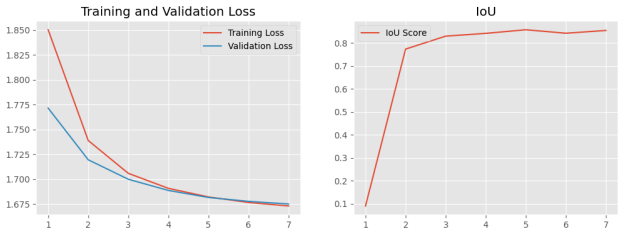

Figure 8. UNET++-Results

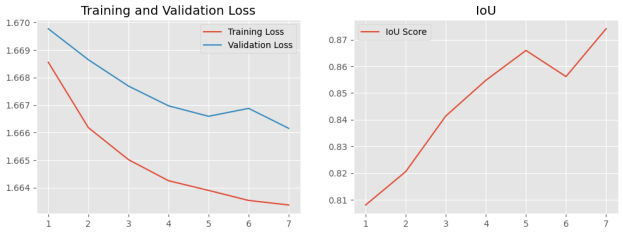

Figure 9. Deeplabv3

Figure 10. PAN-Results

4.2. Classification results

In this section, we show the performance of models within the classification and segmentation tasks.
The table below describes the performance of classification models, which were trained on the original MRI images:

Table 3. Classification Performance on Original Data

Metric	ResNet18	ResNet34	ResNet50	Eff.Net
Train loss	0.446	0.369	0.490	0.295
Val loss	0.424	0.474	0.603	0.255
Train Acc.	0.83	0.86	0.81	0.89
Val Acc.	0.84	0.81	0.79	0.90
Train Prec.	0.82	0.85	0.80	0.88
Val Prec.	0.84	0.82	0.71	0.90
Train Rec.	0.83	0.87	0.81	0.89
Val Rec.	0.83	0.83	0.80	0.90
Train F1	0.81	0.85	0.79	0.87
Val F1	0.83	0.80	0.78	0.89

The table below describes the performance of classification models, which were trained on the combination of MRI images with segmentation masks:

Table 4. Classification Performance on Masked Data

Metric	ResNet18	ResNet34	ResNet50	Eff.Net
Train loss	0.067	0.086	0.212	0.210
Val loss	1.367	2.272	0.759	0.918
Train Acc.	0.98	0.97	0.93	0.94
Val Acc.	0.63	0.58	0.75	0.72
Train Prec.	0.98	0.97	0.93	0.92
Val Prec.	0.64	0.58	0.75	0.72
Train Rec.	0.98	0.97	0.94	0.94
Val Rec.	0.63	0.61	0.74	0.70
Train F1	0.98	0.97	0.93	0.93
Val F1	0.60	0.52	0.72	0.70

According to performance tables, the best result for the classification dataset *EfficientNet* has shown, while for the masked classification dataset the best result was produced by *ResNet50*.

4.2.1. Performance Plots

ResNet18:

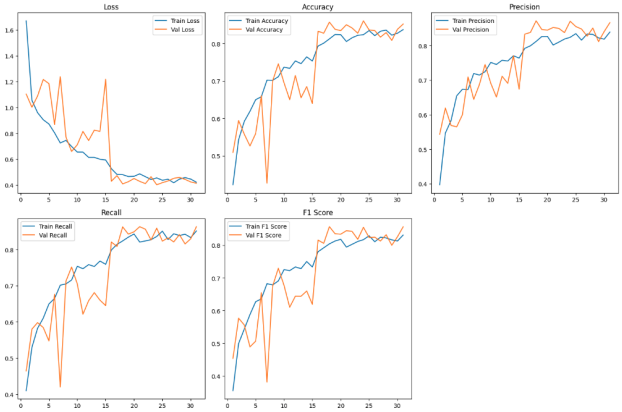

Figure 11. ResNet18 performance on the classification dataset

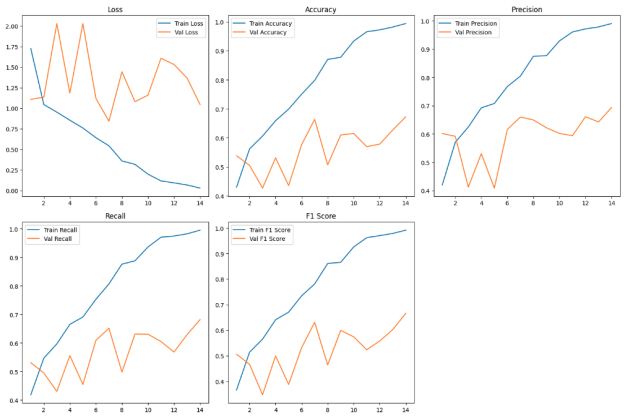

Figure 12. ResNet18 performance on the masked classification dataset

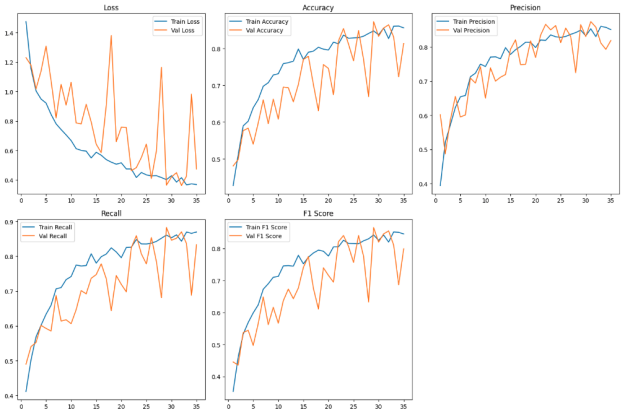

Figure 13. ResNet34 performance on the classification dataset

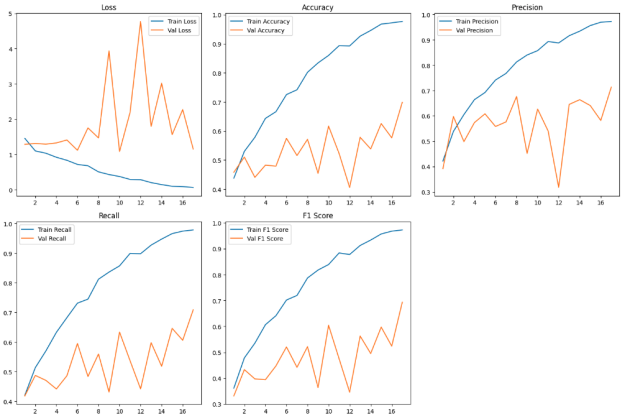

Figure 14. ResNet34 performance on the masked classification dataset

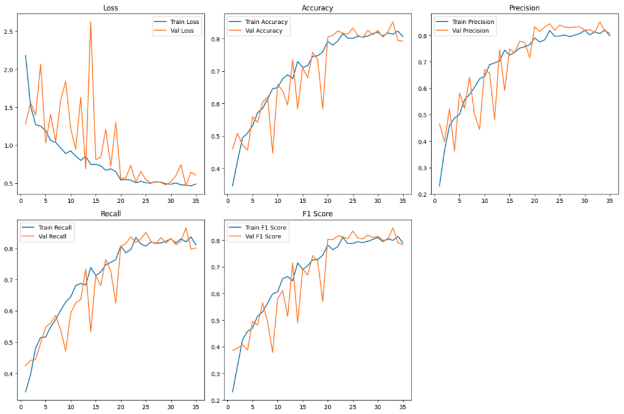

Figure 15. ResNet50 performance on the classification dataset

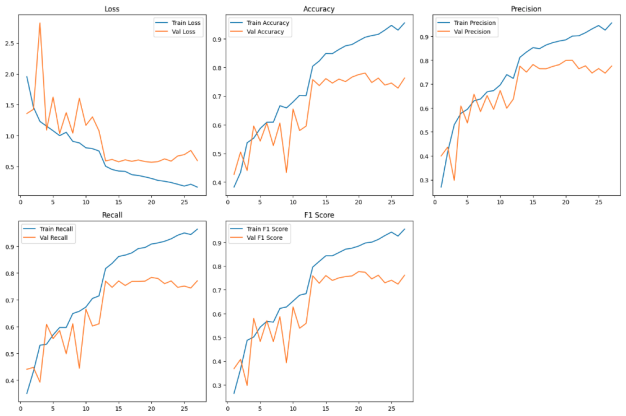

Figure 16. ResNet50 performance on the masked classification dataset

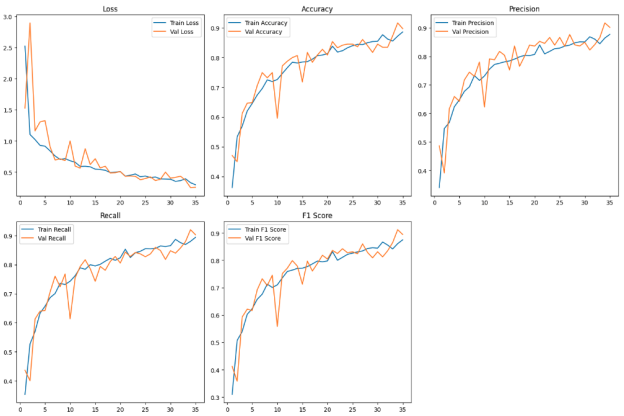

Figure 17. EfficientNet-b0 performance on the classification dataset

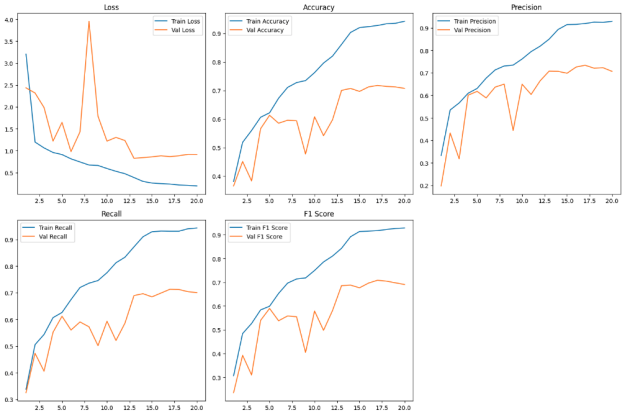

Figure 18. EfficientNet-b0 performance on the masked classification dataset

5. Conclusion

In the current paper, we provide a comparative analysis of classification models' performance. The mentioned hypothesis states that by overlaying segmentation masks on original MRI data we increase the performance of classification models in comparison with leveraging just original MRI images. To evaluate the performance of classification models we use the following metrics: accuracy, precision, recall, and f1 score.

Considering the results of the experiments, our hypothesis was not justified. We got better results on the train set and worse results on the validation set, which looks like overfitting.

The possible reasons for overfitting could be wrong hyperparameters or inaccurate segmentation masks.

6. Team member's contributions

Explicitly stated contributions of each team member to the final project.

Hasaan Maqsood (33% of work)

- Leading the project team
- overseeing all aspects of the project to ensure the quality work
- implementation of project, report and maintain the repository.

Inna Larina (33% of work)

- Implementing classification on original and masked dataset.
- Evaluating classification models' performance and providing plots.
- Writing project plan and team description in early re-

port.

Iana Kulichenko (33% of work)

- Implementing segmentation tasksk
- Feature engineering
- Aiming to accurately identify characteristics that distinguish pituitary tumors in imaging studies.
- Conducting research on contemporary DL models for segmentation task and writing literature review in early report.

7. Reproducibility checklist

Answer the questions of following reproducibility checklist. If necessary, you may leave a comment.

1. A ready code was used in this project, e.g. for replication project the code from the corresponding paper was used.

   ☐ Yes.
   ☑ No.
   ☐ Not applicable.

   General comment: If the answer is **yes**, students must explicitly clarify to which extent (e.g. which percentage of your code did you write on your own?) and which code was used.

   Students' comment: We have used existing PyTorch library for segmentation and then we have fine tune hyper-parameter and then combine for classification

2. A clear description of the mathematical setting, algorithm, and/or model is included in the report.

   ☐ Yes.
   ☑ No.
   ☐ Not applicable.

   Students' comment: None

3. A link to a downloadable source code, with specification of all dependencies, including external libraries is included in the report.

   ☑ Yes.
   ☐ No.
   ☐ Not applicable.

   Students' comment: Everything is mentioned in requirements.txt

4. A complete description of the data collection process, including sample size, is included in the report.

   ☑ Yes.
   ☐ No.
   ☐ Not applicable.

   Students' comment: we have include the complete description of data

5. A link to a downloadable version of the dataset or simulation environment is included in the report.

   ☑ Yes.
   ☐ No.
   ☐ Not applicable.

   Students' comment: Dataset section is link to daataset

6. An explanation of any data that were excluded, description of any pre-processing step are included in the report.

   ☑ Yes.
   ☐ No.
   ☐ Not applicable.

   Students' comment: we have used complete dataset didn't exclude any portion of data

7. An explanation of how samples were allocated for training, validation and testing is included in the report.

   ☑ Yes.
   ☐ No.
   ☐ Not applicable.

   Students' comment: None

8. The range of hyper-parameters considered, method to select the best hyper-parameter configuration, and specification of all hyper-parameters used to generate results are included in the report.

   ☑ Yes.
   ☐ No.
   ☐ Not applicable.

   Students' comment: In order not to lose all the results, we manually sorted through the hyper parameters since training one model takes a very long time

9. The exact number of evaluation runs is included.

   ☑ Yes.
   ☐ No.
   ☐ Not applicable.

   Students' comment:

10. A description of how experiments have been conducted is included.

    ☐ Yes.

- ☐ No.
- ☐ Not applicable.

Students' comment: Please check Results section

11. A clear definition of the specific measure or statistics used to report results is included in the report.

- ☑ Yes.
- ☐ No.
- ☐ Not applicable.

Students' comment:

12. Clearly defined error bars are included in the report.

- ☑ Yes.
- ☐ No.
- ☐ Not applicable.

Students' comment: None

13. A description of the computing infrastructure used is included in the report.

- ☐ Yes.
- ☑ No.
- ☐ Not applicable.

Students' comment: None

References

[1] J. Ma, Y. He, F. Li, L. Han, C. You, and B. Wang, "Segment anything in medical images," *Nature Communications*, vol. 15, no. 1, p. 654, 2024. [Online]. Available: https://doi.org/10.1038/s41467-024-44824-z

[2] D. Xu, X. Zhou, X. Niu, and J. Wang, "Automatic segmentation of low-grade glioma in mri image based on unet++ model," *Journal of Physics: Conference Series*, vol. 1693, no. 1, p. 012135, dec 2020. [Online]. Available: https://dx.doi.org/10.1088/1742-6596/1693/1/012135

[3] H. A. Hafeez, M. A. Elmagzoub, N. A. B. Abdullah, M. S. A. Reshan, G. Gilanie, S. Alyami, M. U. Hassan, and A. Shaikh, "A cnn-model to classify low-grade and high-grade glioma from mri images," *IEEE Access*, vol. 11, pp. 46 283–46 296, 2023.

[4] F. Khan, S. Ayoub, Y. Gulzar, M. Majid, F. A. Reegu, M. S. Mir, A. B. Soomro, and O. Elwasila, "Mri-based effective ensemble frameworks for predicting human brain tumor," *Journal of Imaging*, vol. 9, no. 8, p. 163, 2023.

[5] S. Saeedi, S. Rezayi, H. Keshavarz, and S. R. Niakan Kalhori, "Mri-based brain tumor detection using convolutional deep learning methods and chosen machine learning techniques," *BMC Medical Informatics and Decision Making*, vol. 23, no. 1, p. 16, 2023. [Online]. Available: https://doi.org/10.1186/s12911-023-02114-6

[6] S. Chatterjee, F. A. Nizamani, A. Nürnberger, and O. Speck, "Classification of brain tumours in mr images using deep spatiospatial models," *Scientific Reports*, vol. 12, no. 1, p. 1505, 2022. [Online]. Available: https://doi.org/10.1038/s41598-022-05572-6

[7] D. N. Louis, A. Perry, P. Wesseling, D. J. Brat, I. A. Cree, D. Figarella-Branger, C. Hawkins, H. K. Ng, S. M. Pfister, G. Reifenberger, R. Soffietti, A. von Deimling, and D. W. Ellison, "The 2021 who classification of tumors of the central nervous system: a summary," *Neuro-oncology*, vol. 23, no. 8, pp. 1231–1251, 2021. [Online]. Available: https://doi.org/10.1093/neuonc/noab106

[8] M. Aggarwal, A. K. Tiwari, M. P. Sarathi, and A. Bijalwan, "An early detection and segmentation of brain tumor using deep neural network," *BMC Medical Informatics and Decision Making*, vol. 23, no. 1, p. 78, 2023. [Online]. Available: https://doi.org/10.1186/s12911-023-02174-8

[9] C. G. Bangalore Yogananda, B. R. Shah, M. Vejdani-Jahromi, S. S. Nalawade, G. K. Murugesan, F. F. Yu, M. C. Pinho, B. C. Wagner, K. E. Emblem, A. Bjørnerud, B. Fei, A. J. Madhuranthakam, and J. A. Maldjian, "A fully automated deep learning network for brain tumor segmentation," *Tomography*, vol. 6, no. 2, pp. 186–193, 2020. [Online]. Available: https://doi.org/10.18383/j.tom.2019.00026

[10] M. Ghaffari, A. Sowmya, and R. Oliver, "Automated brain tumor segmentation using multimodal brain scans: A survey based on models submitted to the brats 2012-2018 challenges," *IEEE Reviews in Biomedical Engineering*, vol. 13, pp. 156–168, 2020. [Online]. Available: https://doi.org/10.1109/RBME.2019.2946868

[11] S. Bhuvaji, A. Kadam, P. Bhumkar, S. Dedge, and S. Kanchan, "Brain tumor classification (mri)," 2020. [Online]. Available: https://www.kaggle.com/dsv/1183165